Περιοδικό της Ελληνικής Κτηνιατρικής Εταιρείας

Τόμ. 75, Αρ. 3 (2024)

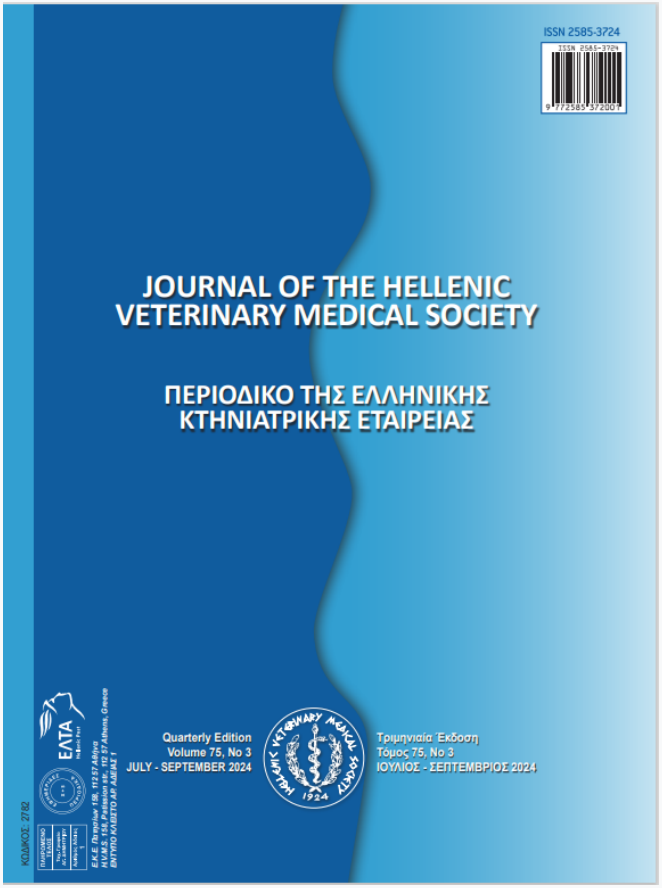

Diagnosis and management of Canine Renal Cell Carcinoma with special reference to Shear Wave Elastography

B Jena, J Mohindroo, A Anand, K Gupta

doi: 10.12681/jhvms.34980

Βιβλιογραφική αναφορά:

Jena, B., Mohindroo, J., Anand, A., & Gupta, K. (2024). Diagnosis and management of Canine Renal Cell Carcinoma with special reference to Shear Wave Elastography. *Περιοδικό της Ελληνικής Κτηνιατρικής Εταιρείας*, *75*(3), 8125–8134. https://doi.org/10.12681/jhvms.34980

J HELLENIC VET MED SOC 2024, 75 (3): 8125-8134
ΠΕΚΕ 2024, 75 (3): 8125-8134

Case report
Κλινικό περιστατικό

Diagnosis and management of canine renal cell carcinoma with special reference to shear wave elastography

B. Jena[1*], J. Mohindroo[1], A. Anand[1], K. Gupta[2]

[1]*Department of Veterinary Surgery and Radiology*

[2]*Department of Veterinary Pathology, College of Veterinary Science, Guru Angad Dev Veterinary and Animal Sciences University, Ludhiana, Punjab, India*

ABSTRACT: This report focuses on the diagnosis and surgical management of unilateral renal cell carcinoma in a 7-year-old male intact German Shepherd dog. The dog was presented with fever, haematuria, inappetence, infrequent bouts of emesis, and progressive weight loss. Palpation revealed a hard, round mass in the right cranial abdomen. A presumptive diagnosis of unilateral renal neoplasm was made based on clinical signs, haematobiochemical analysis, and radiography. B-mode ultrasound examination demonstrated an enlarged right kidney extending up to the ventral midline. The kidney exhibited heterogenous echotexture, loss of renal architecture, and only a small healthy portion at the caudal pole. Point Shear Wave Elastography analysis revealed elevated values both in terms Shear Wave Velocity (m/sec) and Young's Modulus Stiffness Value (kPa), indicating the presence of renal malignancy. To treat the condition, unilateral nephroureterectomy was performed under general anaesthesia. Histopathological examination confirmed the diagnosis of renal cell carcinoma. Consequently, it can be concluded that B-mode ultrasonography, Point Shear Wave Elastography, and nephroureterectomy played crucial roles in the successful diagnosis and surgical management of unilateral renal cell carcinoma.

***Keywords*:** Dog; Nephroureterectomy; Renal Cell Carcinoma; Ultrasound; Shear Wave Elastography.

Corresponding Author:
Biswadeep Jena, Department of Veterinary Surgery and Radiology, Guru Angad Dev Veterinary and Animal Sciences University, Ludhiana, Punjab, India - 141004
E-mail address: biswadeep44@gmail.com

Date of initial submission: 18-07-2023
Date of acceptance: 08-03-2024

CASE HISTORY

Primary renal tumors like renal cell carcinoma (RCC), are of rare yet malignant occurrence, affecting only a small percentage of canine population (Baskin and De Paoli, 1977; Bryan et al., 2006; Darakamas et al., 2022) with a breed predilection among German Shepherds, Labrador Retrievers, Golden Retrievers, and Boxers (Meuten and Meuten, 2016). These tumors tend to manifest in more in male dogs who are typically middle-aged or older (Lucke and Kelly, 1976; Baskin and De Paoli, 1977; Klein et al., 1988; Bryan et al., 2006; Chiang et al., 2007; Edmondson et al., 2015). Adjuvant chemotherapy, despite its disappointing results in human cases, has not been extensively explored as a treatment option for primary renal tumors in dogs, leaving surgical intervention as the primary choice to improve prognosis (Klein et al., 1988; Bryan et al., 2006; Carvalho et al., 2017).

Studies have revealed the remarkable functional reserves of canine kidneys (Finco et al., 1999). It has been observed that levels of serum creatinine (sCr), a widely used surrogate biomarker for renal function in developing countries, rise beyond the normal range only when there is a 75% loss of functional renal mass or a 40% reduction in glomerular filtration rate (GFR) (Cobrin et al., 2013; Relford et al., 2016). By the time cases with renal impairment are presented, the irreversible loss suffered by the kidneys' reserves often leads to a guarded to poor prognosis and a subsequent decrease in survival time.

The timely diagnosis of renal diseases and renal failure in dogs is of utmost importance to initiate therapeutic or surgical interventions that can potentially slow down or halt disease progression (Lees, 2004). Diagnostic imaging modalities, including radiography (Edmondson et al., 2015; Darakamas et al., 2022), B-mode ultrasound (Bryan et al., 2006; Edmondson et al., 2015), colour Doppler ultrasonography (Chen et al., 2021), and CT scan (Darakamas et al., 2022; Noh et al., 2022), have played a crucial role in detecting primary renal tumors. However, since CT scan availability may be limited in some centers, techniques such as radiography, B-mode ultrasound, and color Doppler ultrasonography can only provide a qualitative assessment of renal lesions. This limitation renders them unreliable for definitive differential diagnosis and evaluating the progression of renal diseases. Renal biopsy (Rawlings et al., 2003) and fine needle aspiration cytology (FNAC) (McAloney et al., 2018) have been regarded as the gold standard for assessing the advancement of renal conditions. Unfortunately, these invasive techniques come with complications, including a 5.5% incidence of discrete light microscopic lesions and visible capsular scars in canine patients undergoing biopsy or FNAC (Groman et al., 2004).

Ultrasound-based Point Shear Wave Elastography (pSWE), which holds promise as a potential imaging technique. This innovative approach measures the stiffness of tissues or regions of interest under scrutiny, serving as a valuable aid in differential diagnosis and the assessment of renal disease progression (Bob et al., 2017).

This communication aimed to evaluate the clinical manifestations, laboratory findings, and the impact of various diagnostic modalities and surgical interventions on the successful recovery of a dog with unilateral renal cell carcinoma.

Over a span of two years, from May 2021 to May 2023, a total of 198 dogs of varied age, breed, gender, and body weight, suspected with renal diseases were enrolled in this study. Among these cases, we identified a single instance of unilateral renal cell carcinoma based on a combination of clinical signs, hematological findings, renal function tests, routine urinalysis observations, radiography, B-mode ultrasonography, point shear wave elastography (pSWE), surgical intervention, and histopathology.

The affected dog was a 7-year-old intact male German Shepherd, weighing 24 kg, with a body condition score of 2.5. The dog was presented with symptoms such as fever (38.9 °C), tachycardia (104 beats per minute), dehydration (8%), chronic hematuria, loss of appetite, occasional vomiting, and progressive weight loss. During physical examination, a hard, round mass was palpated in the right cranial quadrant of the abdomen.

Hematological analysis revealed a normal hemoglobin level (13.2 g/dL), a slight decrease in total erythrocyte count (TEC; 5.39 x 10^6/µL), packed cell volume (PCV; 35.7%), and platelet count (167 x 10^3/µL). Neutrophilic leukocytosis with a mild left shift was also observed (total leukocyte count - 28,000/µL, relative neutrophil count - 88%, and absolute neutrophil count - 24,640). Biochemical analysis showed normal serum creatinine (sCr) levels (1.3 mg/dL), but elevated blood urea nitrogen (BUN) levels (62 mg/dL) and hyperphosphatemia (7.3 mg/dL). Routine

urinalysis revealed increased levels of urinary leukocytes (3+), RBCs (3+), protein (3+), and a high pH (8.5). A decrease in urine specific gravity (1.015) was also observed.

Upon performing orthogonal thoracic radiography, normal cardiopulmonary structures were observed. However, orthogonal abdominal radiographic views revealed a roundish, radiopaque mass occupying a space in the right cranial abdomen, causing dorsal and medial displacement of the gas-filled duodenum (Figure 1).

For further evaluation, B-mode ultrasonography was performed using an ultrasound machine (Make: Philips, Model: Affiniti 70G, Release 2.0.1, Philips Healthcare, 3000 Minuteman Road, Andover, Massachusetts, 01810, United States of America) equipped with linear (C12-5, Philips Healthcare) and curvilinear (C5-1 PureWave, Philips Healthcare) array transducers. For imaging the mass, the curvilinear array transducer (1.0 - 5.0 MHz, depth: 16 cm, gain: 62dB) was utilized, maintaining TIS (Thermal Index for Soft Tissue) at 0.5 and MI (Mechanical Index) at 0.8 for patient safety. For imaging the contralateral healthy

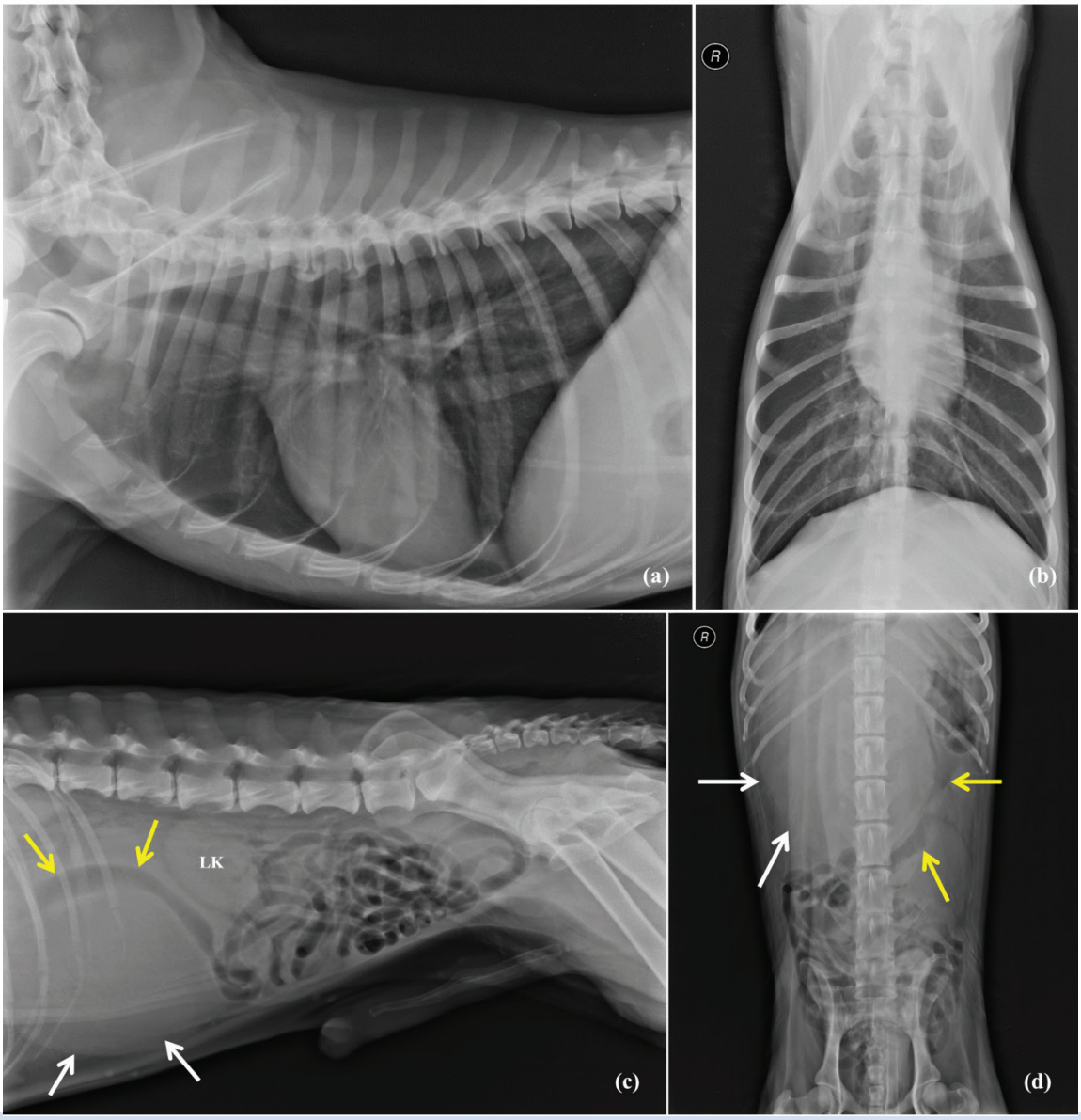

Figure 1. Showing right lateral and ventrodorsal radiographic views of thoracic and abdominal cavity. (a, b) orthogonal thoracic radiographic views revealed normal cardiopulmonary structures; (c, d) orthogonal abdominal radiographic views revealed a radiopaque roundish space occupying lesion (white arrows) present in the right cranial abdomen pushing gas filled duodenum dorsally and medially (yellow arrows). LK = left kidney

kidney, the linear array transducer (5.0 - 12.0 MHz, depth: 8 cm, gain: 63dB) was used, with TIS at 0.0 and MI at 0.7. Adequate frequency was chosen automatically by the ultrasound scanner to balance between sufficient tissue penetration and adequate resolution for precise characterization of the tumor.

The B-mode ultrasonography findings revealed a significantly enlarged right kidney, extending up to the ventral midline, with noticeable loss of renal architecture. The renal parenchyma exhibited heterogeneous echotexture, and anechoic cavitation was detected in the cranial pole of the right kidney. Interestingly, a small, unaffected portion of the kidney was observed at the caudal pole, indicating the presence of a space-occupying lesion originating from the renal tissue. On the other hand, the B-mode ultrasonography of the left kidney showed normal renal architecture (Figure 2).

To enhance visualization and accurately localize the lesions, "iSlice" intelligent slicing technology was performed (Li et al., 2012; Wei et al., 2013; Dong et al., 2016; Song et al., 2018). This technique involved capturing images at various levels in a longitudinal plane, essentially creating "slices" of the space-occupying lesion. These slices were then arranged together in a single frame, facilitating improved visualization and precise localization of the lesions. Notably, no normal renal architecture was identified in any of the slices obtained using iSlice (Figure 3).

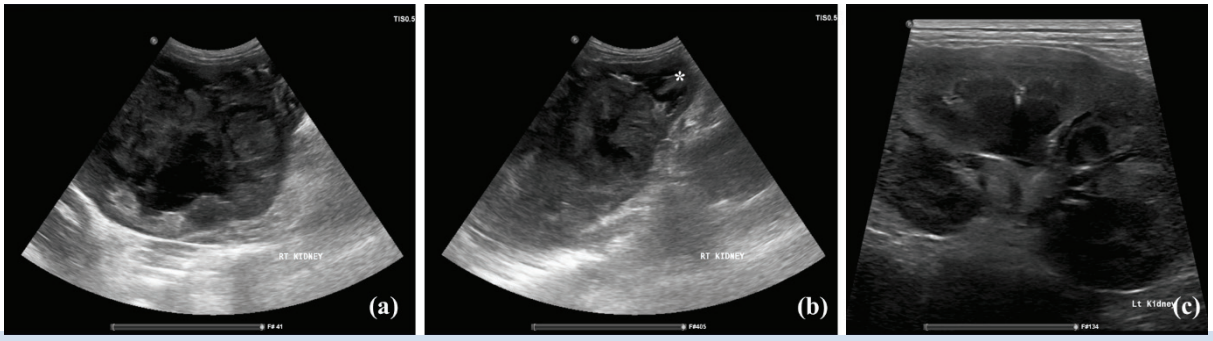

Figure 2. B-mode ultrasonography revealed (a) markedly enlarged right with loss of renal architecture, heterogenous echotexture of renal parenchyma with anechogenic cavitation involving cranial pole of right kidney; (b) a small and healthy part of kidney was observed at the caudal pole of the right kidney (*), suggestive of space occupying lesion of right renal origin; (c) B-mode ultrasonography revealed normal renal architecture of left kidney.

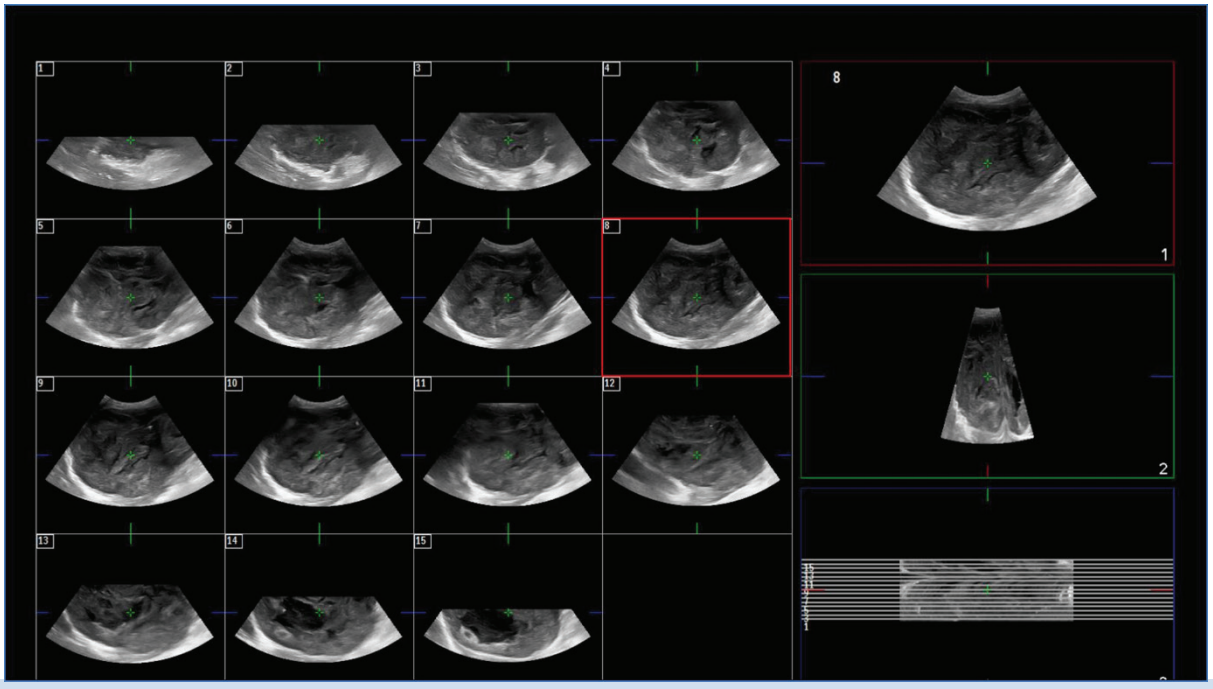

Figure 3. iSlice could not find normal renal architecture in any slice.

In order to conduct pSWE, the 1.0 - 5.0 MHz curvilinear array transducer (C5-1 PureWave, Philips Healthcare) and ElastPQ (EPQ) Stiffness software integrated into the ultrasound scanner were utilized. The dog was positioned in dorsal recumbency with a positioner for optimal imaging. Real-time B-mode combined with pSWE assessed the kidneys, with a fixed rectangular region of interest (ROI) box placed on the cranial and caudal poles of the renal cortex. The ROI had a fixed size and could be moved within the image to a maximum depth of 8 cm, gain set at 60 dB, TIS maintained at 0.4, and MI at 1.3 for patient safety.

Care was taken to avoid overlap with the renal capsule, medulla, blood vessels, cysts, renal sinus, perirenal fat, or surrounding tissues. The operator applied minimal compression during the procedure.

For each kidney, five valid measurements were obtained from both the cranial and caudal poles, and these measurements were combined. The "median" value of the combined measurements was considered as the pSWE value for the respective kidney, following the guidelines established by the World Federation of Ultrasound in Medicine and Biology (WFUMB) and the European Federation of Societies for Ultrasound in Medicine and Biology (EFSUMB) (Iyama et al., 2021; Ferraioli et al., 2022). In this study, the pSWE values were reported in terms of Shear Wave Velocity (SWV) measured in m/sec and Young's Modulus Stiffness Value (YMSV) measured in kPa.

The pSWE study revealed higher values for the suspected tumorous renal mass compared to the healthy contralateral kidney. The median SWV value for the tumorous renal mass was 3.06 m/sec, notably higher than the contralateral healthy kidney's median SWV value of 0.86 m/sec. Similarly, the median YMSV for the tumorous renal mass was 28.49 kPa, notably higher than the contralateral healthy kidney's median YMSV value of 2.43 kPa. These findings strongly suggested the presence of renal malignancy (Figure 4).

Based on the clinical signs, laboratory findings, radiographic, B-mode ultrasonographic, and pSWE studies, a presumptive diagnosis of unilateral renal neoplastic mass was reached. Recognizing that surgery offered the best chance for resolution, it was

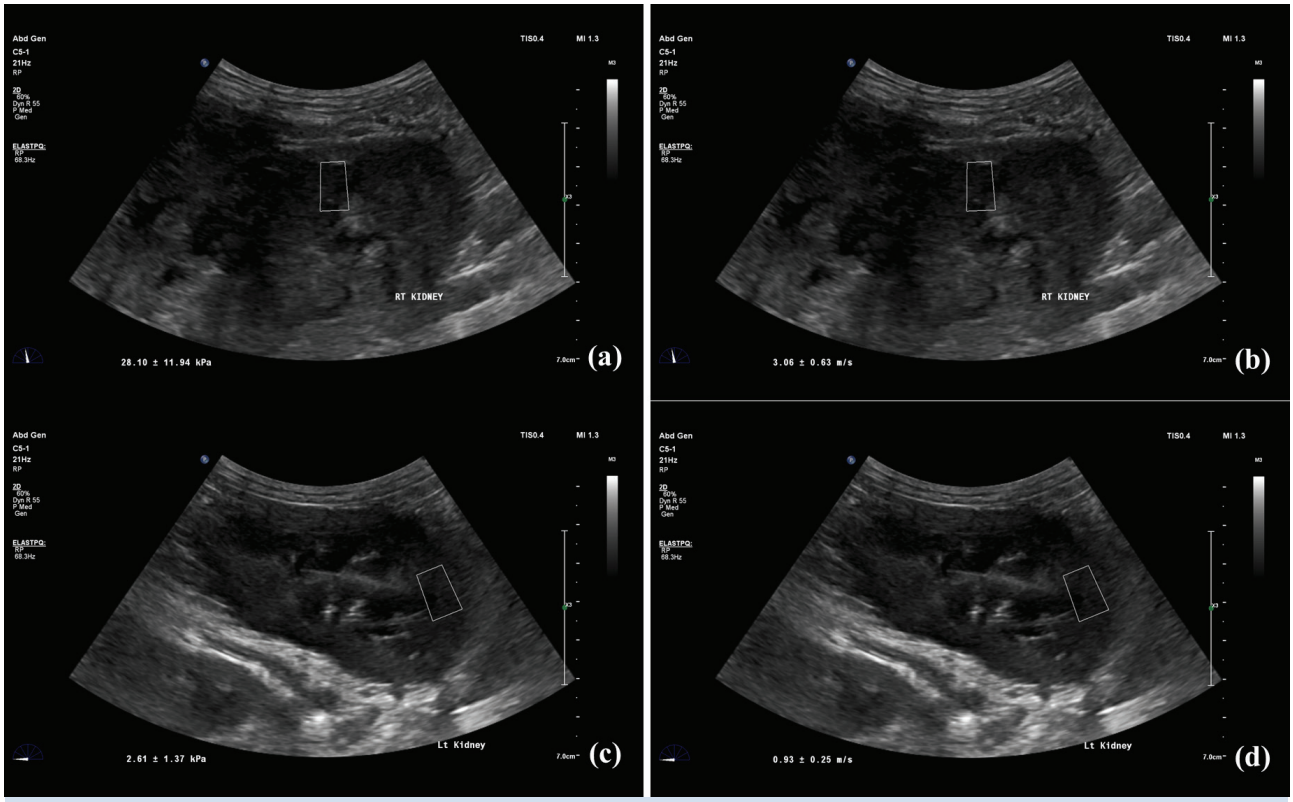

Figure 4. pSWE study revealed higher pSWE values (both in terms of SWV in m/sec and YMSV in kPa) of presumptively malignant renal tumour (a, b) as compared to contralateral healthy kidney (c, d).

decided to proceed with exploratory laparotomy and unilateral nephroureterectomy on the subsequent day. Prior to the surgery, the animal received a premedication cocktail consisting of Butorphanol (Butodol®, Neon at 0.2 mg/kgb.w.), Acepromazine (Acepromazine, VetOne at 0.05 mg/kgb.w.), and Glycopyrrolate (Pyrolate®, Neon at 0.01 mg/kgb.w.) via intramuscular injection. General anesthesia was induced using intravenous Propofol (Neorof®, Neon at 4.0 mg/kgb.w.), followed by endotracheal intubation and maintenance of anesthesia with Isoflurane inhalation. Perioperative fluid therapy was provided, and the routine procedure of unilateral nephroureterectomy was performed through a ventral midline celiotomy as describe by MacPhail (2013). During the exploration, thorough examination of other abdominal organs was conducted to rule out visceral metastasis. Following the nephroureterectomy, the dimensions of the removed kidney were measured, revealing a length of 19.5 cm, width of 14.5 cm, and height of 18.7 cm, with a weight of 1.1 kg (Figure 5). Samples from the mass were collected for histopathological investigation.

In the post-operative period, the dog received fluid therapy (Ringer's lactate, 500 ml intravenously once daily for 3 days), antibiotics (Ceftriaxone and Tazobactam combination, Intacef Tazo®562.5 mg, Intas intravenously, BID for 5 days, and Amikacin, Mikacin®, Aristo 250 mg intramuscularly, OD for 3 days), analgesics (Meloxicam, Melonex®, Intas 5 mg intramuscularly once daily for 3 days), and proton pump inhibitors (Pantoprazole, Pantop®, Aristo at 40 mg intravenously, OD for 3 days). The pet parents were advised to provide the dog with light food until the post-operative suture removal. The cutaneous sutures were later removed on 14th post-operative day and the wound healed without any complications. On the 50th day of post-operative follow-up, the animal appeared healthy with no signs of metastasis (Figure 6).

Histopathological investigation of the mass revealed a significant proliferation of epithelial cells within the kidney tubules. The neoplastic cells exhibited tubular arrangements and, in some areas, formed papillary projections within the tubule lumens. Additionally, there was a proliferation of connective tissue between the neoplastic cells. These histopathological findings confirmed the presence of "Renal Cell Carcinoma" (Figure 7).

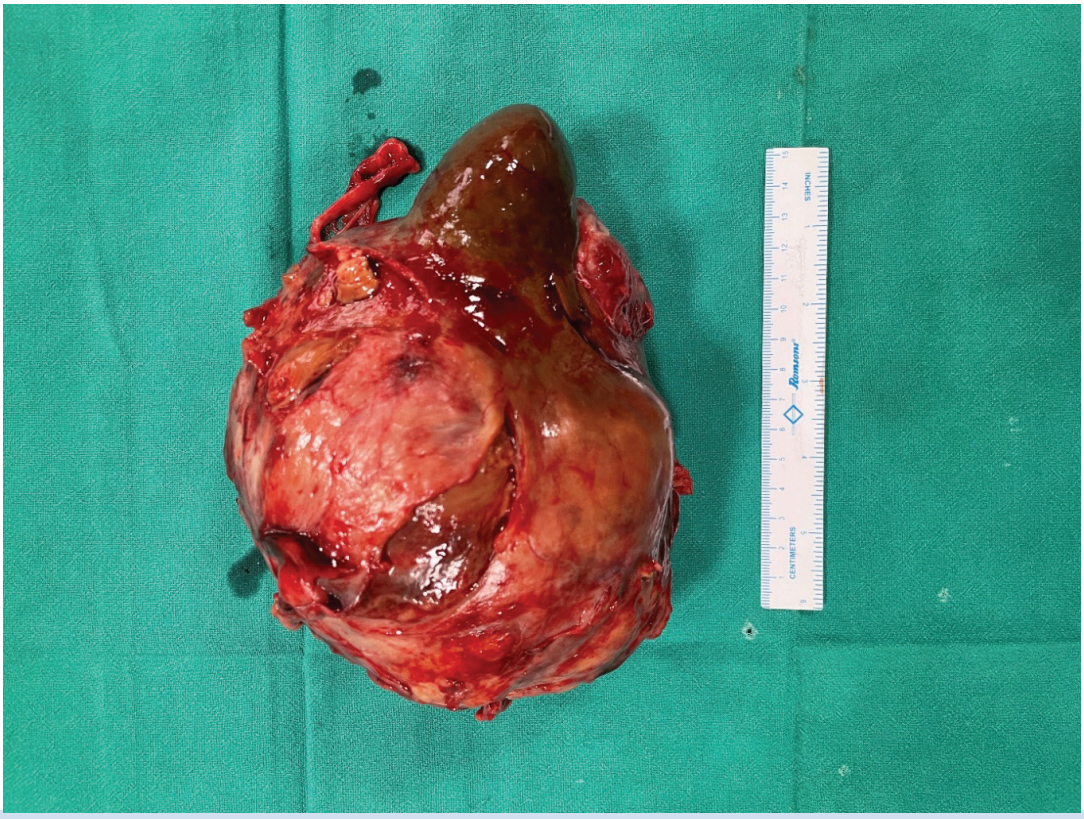

Figure 5. Gross image of renal mass after unilateral nephroureterectomy through ventral midline celiotomy

Figure 6. Uneventful recovery on 50th post-operative day follow-up

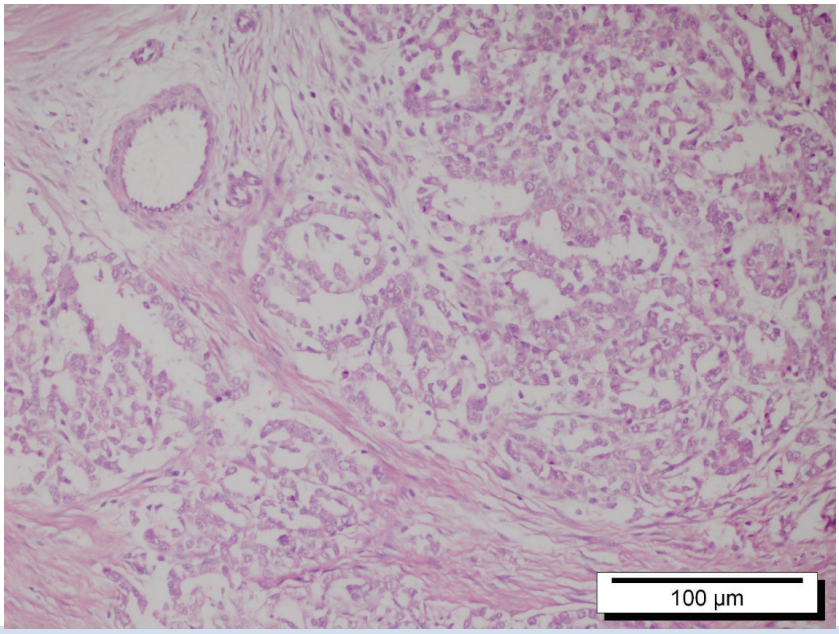

Figure 7. Histopathology suggestive of Renal cell carcinoma (H&E, 20x)

DISCUSSION

According to published reports, dogs between the ages of 7.1 and 8.8 years were found to be more susceptible to renal cell carcinoma (Lucke and Kelly, 1976; Klein et al., 1988; Bryan et al., 2006), which aligns with the age of the dog in this case study. The prevalence of RCC in our sample size was 0.505%, consistent with previous reports (Baskin and De

Paoli, 1977; Bryan et al., 2006). Unilateral RCC presentations were commonly observed (Bryan et al., 2006; Darakamas et al., 2022). Similar to reports by Edmondson et al. (2015) and Darakamas et al. (2022), German Shepherd dogs, retrievers, and boxers were predisposed to RCC.

Clinical signs such as haematuria, inappetence, infrequent bouts of emesis, and progressive weight loss were observed in our study, aligning with previous reports where similar non-specific clinical signs were commonly presented (Lucke and Kelly, 1976; Bryan et al., 2006; Darakamas et al., 2022). Fever was also reported by Bennett (2004), possibly due to paraneoplastic syndrome concurrent with paraneoplastic leukocytosis caused by neoplastic cell elaboration of cerebrospinal fluid (Petterino et al., 2011).

Neutrophilia (20%), anemia (33%), and thrombocytopenia (9%) were less common hematological abnormalities in dogs with primary renal neoplasia (Bryan et al., 2006; Chiang et al., 2007), consistent with the findings of this study. Anemia was not observed, but a mild decrease in total erythrocyte count (TEC) and packed cell volume (PCV) was noted, as reported by Darakamas et al. (2022). This may be attributed to increased release of erythropoietin by the renal mass to maintain hemoglobin levels within the normal physiological range (Waters and Prueter, 1988; Bennett, 2004; Meuten and Meuten, 2016). Neutrophilic leukocytosis, although uncommon, may be due to paraneoplastic leukocytosis, as reported by Petterino et al. (2011).

As reported by Caravalho et al. (2017), 16-19% of canine patients with RCC exhibited elevated serum creatinine (sCr) and blood urea nitrogen (BUN), explaining the lack of sCr elevation in this study, consistent with previous reports by Darakamas et al. (2022). According to Cobrin et al. (2013) and Relford et al. (2016), sCr levels would only increase beyond the biological reference range with more than 75% irreversible loss of functional units of kidney. This suggests that the case in this study presented at an early stage, with some renal functional reserve still intact, indicating a favorable prognosis.

Routine urinalysis commonly revealed hematuria, proteinuria, and pyuria, as reported by Bryan et al. (2006), Petterino et al. (2011), and Darakamas et al. (2022), which aligns with our findings. Bryan et al. (2006) also reported isosthenuria as a common finding in routine urinalysis. Although isosthenuria was not observed in our study, a decrease in urinary specific gravity was noted, indicating mild impairment of the kidney, in corroboration with findings of Darakamas et al. (2022).

According to Bryan et al. (2006) and Noh et al. (2022), primary renal neoplasms like RCC often have metastatic properties, with pulmonary metastasis observed in 16 to 26.7% of dogs. Chiang et al. (2007) reported RCC metastasis to hypertrophic osteopathy. However, orthogonal thoracic radiography in this case study revealed a normal lung pattern, suggesting the absence of metastasis. Orthogonal abdominal radiographs aided in localizing and approximating the size of the space-occupying mass, revealing a radiopaque silhouette. However, a lateral abdominal radiograph raised doubts due to the dorsal deviation of the gas-filled duodenum, mimicking a space-occupying lesion originating from the splenic parenchyma. B-mode ultrasonography, on the other hand, confirmed the origin of the mass in the right kidney and the loss of internal renal architecture. It also helped in confirming the absence of metastasis to other abdominal organs. iSlice was unable to visualize the unaffected portion of right kidney which might be due to big size of the mass and different plane of scan.

There was a lack of supporting literature in veterinary medicine regarding SWE based evaluation of renal mass. But in human medicine, previous reports have explored the efficacy of SWE in evaluating kidney masses (Iyama et al., 2021). Göya et al. (2015) conducted a study to distinguish between benign and malignant kidney tumors in humans, where the malignant tumors showed higher SWE values. Another study involving 197 human patients with kidney lesions demonstrated significantly higher SWV in cases of renal cell carcinoma (Lu et al., 2015). Consistent with these findings, the SWV and YMSV of RCC in this case were higher compared to the contralateral healthy kidney. The elevated pSWE values can be attributed to the proliferation of neoplastic cells in a confined area, resulting in increased stiffness of the RCC. Histopathological findings were in agreement with previous reports (Chiang et al., 2007; Petterino et al., 2011; Edmondson et al., 2015; Meuten and Meuten, 2016)

To the best of the authors knowledge, no report was available on the role of pSWE in the differential diagnosis of renal cell carcinoma in dogs at the time of writing of this manuscript. So, the present report puts on record that the elevated Shear Wave Elastography

Velocity and loss of renal architecture, supported by histopathological findings, confirmed the diagnosis of "Renal Cell Carcinoma." Nephrectomy proved to be an effective treatment for renal carcinoma in this case. Since the case was detected at an early stage, following proper diagnostic and surgical techniques resulted in an uneventful recovery and improved survival time for the animal.

ACKNOWLEDGMENT

Authors were thankful to Indian Council of Agricultural Research - All India Network Program on "Diagnostic Imaging and Management of Surgical Conditions in Animals" and Guru Angad Dev Veterinary and Animal Sciences University, Ludhiana, Punjab for their support in terms of various resources for conducting this research.

CONFLICT OF INTEREST

None declared

ANIMAL WELFARE

The study was approved by the Institutional Animal Ethics Committee (IAEC), Guru Angad Dev Veterinary and Animal Sciences University (GADVASU), Ludhiana vide proposal number GADVASU/2021/IAEC/59/12.

REFERENCES

Baskin GB, De Paoli A (1977) Primary Renal Neoplasms of the Dog. Vet Pathol 14:591-605. https://doi.org/10.1177/030098587701400606

Bennett F (2004) Unilateral renal cell carcinoma in a Labrador retriever. Can Vet J 45:860- 862. https://pubmed.ncbi.nlm.nih.gov/15532889

Bob F, Grosu I, Sporea I, Bota S, Popescu A, Sima A, Şirli R, Petrica L, Timar R, Schiller A (2017) Ultrasound-based shear wave elastography in the assessment of patients with diabetic kidney disease. Ultrasound Med Biol 43:2159-2166. https://doi.org/10.1016/j.ultrasmedbio.2017.04.019

Bryan JC, Henry CJ, Turnquist SE, Tyler JW, Liptak JM, Rizzo SA, Sfiligoi G, Steinberg SJ, Smith AN, Jackson T (2006) Primary Renal Neoplasia of Dogs. J Vet Intern Med. 20:1155-1160. https://doi.org/10.1111/j.1939-1676.2006.tb00715.x

Carvalho S, Stoll AL, Priestnall SL, Suarez-Bonnet A, Rassnick K, Lynch S, Schoepper I, Romanelli G, Buracco P, Atherton M, De Merlo EM (2017) Retrospective evaluation of COX-2 expression, histological and clinical factors as prognostic indicators in dogs with renal cell carcinomas undergoing nephrectomy. Vet Comp Oncol 15:1280-1294. https://doi.org/10.1111/vco.12264

Chen M, Fu X, Shen Y(2021) Evaluation of multimode color doppler flow imaging in the diagnosis of solid renal tumor. Contrast Media Mol Imaging2021:1-7. https://doi.org/10.1155/2021/6656877

Chiang YC, Liu CH, Ho SY, Lin CT, Yeh LS (2007) Hypertrophic osteopathy associated with disseminated metastases of renal cell carcinoma in the dog: a case report. J Vet Med 69:209-212. https://doi.org/10.1292/jvms.69.209

Cobrin AR, Blois SL, Kruth SA, Abrams-Ogg AC, Dewey C (2013) Biomarkers in the assessment of acute and chronic kidney diseases in the dog and cat. J Small Anim Pract. 54:647-655. https://doi.org/10.1111/jsap.12150

Darakamas P, Chandrasakha P, Suwannaprapha P, Banjathammarak S, Chuaychoo K, Kongtasai T. Clear Cell Renal Cell Carcinoma in a Dog. J Appl Anim Res 15:51-64.

Dong F, Xu J, Du D, Jiao Y, Zhang L, Li M, Liu H, Xiong Y, Luo H(2016) 3D analysis is superior to 2D analysis for contrast-enhanced ultrasound in revealing vascularity in focal liver lesions-A retrospective analysis of 83 cases. Ultrasonics 70: 221-226.https://doi.org/10.1016/j.ultras.2016.05.007

Edmondson EF, Hess AM, Powers BE. (2015) Prognostic Significance of Histologic Features in Canine Renal Cell Carcinomas. Vet Pathol 52: 260-268. https://doi.org/10.1177/0300985814533803

Ferraioli G, Barr RG, Farrokh A, Radzina M, Cui XW, Dong Y, Rocher L, Cantisani V, Polito E, D'Onofrio M, Roccarina D (2022) How to perform shear wave elastography. Part II. Med Ultrason 24:196-210. https://doi.org/10.11152/mu-3342

Finco DR, Brown SA, Brown CA, Crowell WA, Cooper TA, Barsanti JA (1999) Progression of chronic renal disease in the dog. J Vet Intern Med 13:516-528. https://doi.org/10.1111/j.1939-1676.1999.tb02204.x

Göya C, Daggulli M, Hamidi C, Yavuz A, Hattapoglu S, Cetincakmak MG, Teke M (2015) The role of quantitative measurement by acoustic radiation force impulse imaging in differentiating benign renal lesions from malignant renal tumours. La Radiologia Medica 120:296-303. https://doi.org/10.1007/s11547-014-0443-7

Groman RP, Bahr A, Berridge BR, Lees GE (2004) Effects of serial ultrasound-guided renal biopsies on kidneys of healthy adolescent dogs.Vet Radiol Ultrasound 45:62-69. https://doi.org/10.1111/j.1740-8261.2004.04010.x

Iyama T, Sugihara T, Takata T, Isomoto (2021) Renal Ultrasound Elastography: A Review of the Previous Reports on Chronic Kidney Diseases. Appl Sci 11:9677. https://doi.org/10.3390/app11209677

Klein MK, Cockerell GL, Harris CK, Withrow SJ, Lulich JP, Ogilvie GK, Norris AM, Harvey HJ, Richardson RF, Fowler JD (1988) Canine primary renal neoplasms: a retrospective review of 54 cases. J Am Anim Hosp Assoc 24:443-452. https://agris.fao.org/agris-search/search.do?recordID=US8857240

Lees GE (2004) Early diagnosis of renal disease and renal failure. Vet Clin North Am Small Anim Pract 34:867-885. https://doi.org/10.1016/j.cvsm.2004.03.004

Li QY, Tang J, He EH, Li YM, Zhou Y, Zhang X, Chen G (2012) Clinical utility of three-dimensional contrast-enhanced ultrasound in the differentiation between noninvasive and invasive neoplasms of urinary bladder. EurJRadiol 81: 2936-2942.https://doi.org/10.1016/j.ejrad.2011.12.024

Lu Q, Wen JX, Huang BJ, Xue LY, Wang WP (2015) Virtual Touch quantification using acoustic radiation force impulse (ARFI) technology for the evaluation of focal solid renal lesions: preliminary findings. Clin Radiol 70:1376-1381. https://doi.org/10.1016/j.crad.2015.08.002

Lucke VM, Kelly DJ (1976) Renal Carcinoma in the Dog. Vet Pathol 13:264-276. https://doi.org/10.1177/030098587601300403

MacPhail CM (2013) Surgery of the kidney and ureter. In: Fossum TW editor. Small Animal Surgery. 4th ed, Elsevier, pp. 705-734.

McAloney CA, Sharkey LC, Feeney DA, Seelig DM, Avery AC, Jessen CR (2018) Evaluation of the diagnostic utility of cytologic examination of renal fine-needle aspirates from dogs and the use of ultrasonographic features to inform cytologic diagnosis. J Am Vet Med Assoc

252:1247-1256. https://doi.org/10.2460/javma.252.10.1247
Meuten DJ, Meuten TL (2016) Tumors of the urinary System. In: Meuten DJ editor. Tumors in domestic animals. 5th ed, John Wiley & Sons. Inc. Publishing, Ames: pp 632-688.
Noh D, Shim J, Choi S, Choi H, Lee Y, Lee K (2022) Computed tomographic findings of primary renal tumors in dogs and cats. Thai J Vet Med 52:499-505. https://digital.car.chula.ac.th/tjvm/vol52/iss3/8
Noh D, Shim JW, Choi S, Choi H, Lee Y, Lee K (2022) Computed tomographic findings of primary renal tumors in dogs and cats. Thai J Vet Med52:499-505. https://doi.org/10.56808/2985-1130.3242
Petterino C, Luzio E, Baracchini L, Ferrari AP, Ratto A (2011) Paraneoplastic leukocytosis in a dog with a renal carcinoma. Vet Clin Pathol 40:89-94. https://doi.org/10.1111/j.1939-165x.2011.00296.x
Rawlings CA, Diamond H, Howerth EW, Neuwirth L, Canalis C (2003) Diagnostic quality of percutaneous kidney biopsy specimens obtained with laparoscopy versus ultrasound guidance in dogs. J Am Vet Med Assoc 223: 317- 321. https://doi.org/10.2460/javma.2003.223.317
Relford R, Robertson J, Clements C (2016) Symmetric dimethylarginine: improving the diagnosis and staging of chronic kidney disease in small animals. Vet Clin North Am Small Anim Pract 46:941-960. https://doi.org/10.1016/j.cvsm.2016.06.010
Song Y, Cheng J, Zhang R (2018) Contribution of 3-Dimensional Contrast-Enhanced Ultrasonography (CEUS) Compared With 2-Dimensional CEUS in the Analysis of Liver Tumors. J Ultrasound Med37: 1117-1128.https://doi.org/10.1002/jum.14458
Waters D, Prueter JC. (1988) Secondary polycythemia associated with renal disease in the dog: two case reports and review of literature. J Am. Anim Hosp Assoc 24:109-114.
Wei S, Fu N, Yao C, Liu P, Yang B (2013) Two-and Three-Dimensional Contrast-Enhanced Sonography for Assessment of Renal Tumor Vasculature: Preliminary Observations. J Ultrasound Med 32: 429-437. https://doi.org/10.7863/jum.2013.32.3.429